J Biomol NMR (2012) 53:303–310
DOI 10.1007/s10858-012-9640-7

ARTICLE

A 2D ^{13}C-CEST experiment for studying slowly exchanging protein systems using methyl probes: an application to protein folding

Guillaume Bouvignies · Lewis E. Kay

Received: 6 April 2012 / Accepted: 23 May 2012 / Published online: 12 June 2012

Abstract A 2D ^{13}C Chemical Exchange Saturation Transfer (CEST) experiment is presented for studying slowly exchanging protein systems using methyl groups as probes. The utility of the method is first established through studies of protein L, a small protein, for which chemical exchange on the millisecond time-scale is not observed. Subsequently the approach is applied to a folding exchange reaction of a G48M mutant Fyn SH3 domain, for which only cross-peaks derived from the folded ('ground') state are present in spectra. Fits of ^{15}N and methyl ^{13}C CEST profiles of the Fyn SH3 domain establish that the exchange reaction involves an interchange between folded and unfolded conformers, although elevated methyl ^{13}C transverse relaxation rates for some of the residues of the unfolded ('invisible, excited') state indicate that it likely exchanges with a third conformation as well. In addition to the kinetics of the exchange reaction, methyl carbon chemical shifts of the excited state are also obtained from analysis of the ^{13}C CEST data.

Keywords Slow chemical exchange · Protein folding · Saturation transfer · Excited protein conformational states · Methyl groups

Introduction

Chemical exchange saturation transfer experiments, originally developed by Forsen and Hoffman in the early 1960s (Forsen and Hoffman 1963), have become a valuable tool for the study of the kinetics of exchanging systems (Alger and Shulman 1984; Cayley et al. 1979; Fawzi et al. 2011; Gupta and Redfield 1970; Ward et al. 2000; Zhou and van Zijl 2006). The basic experiment makes use of a weak radio frequency (rf) field applied at the resonance position of an exchanging spin of interest. The perturbation introduced is transferred to the exchanging site ('acceptor'), and the time dependence of the magnetization provides valuable information on the kinetics of exchange as well as the longitudinal relaxation time of the 'acceptor'. Although very early applications involved small chemical systems in exchange (Forsen and Hoffman 1963), the potential of the method for studies of much larger biomolecules was soon realized with the pioneering studies of Gupta and Redfield who used a saturation transfer based experiment to study electron exchange between oxidized and reduced cytochrome c in a solution containing approximately equally mixtures of both forms of the protein (Gupta and Redfield 1970). These authors also showed that it is possible to correlate the positions of some of the methyl groups of the diamagnetic and paramagnetic states by exploiting the hyperfine shifted methyls in the oxidized conformer and transferring what these authors referred to as 'bleaching' from these moieties to the corresponding groups in the reduced state. Subsequently, the Mill Hill group carried out similar studies of

Electronic supplementary material The online version of this article (doi:10.1007/s10858-012-9640-7) contains supplementary material, which is available to authorized users.

G. Bouvignies · L. E. Kay (✉)
Departments of Molecular Genetics, Biochemistry and Chemistry, The University of Toronto, Toronto, ON M5S 1A8, Canada
e-mail: kay@pound.med.utoronto.ca

L. E. Kay
Hospital for Sick Children, Program in Molecular Structure and Function, 555 University Avenue, Toronto, ON M5G 1X8, Canada

cofactors and inhibitors of the enzyme dihydrofolate reductase, utilizing a saturation transfer effect to obtain the chemical shifts of the bound ligands from experiments monitoring the intensities of well resolved peaks derived from the free state (Cayley et al. 1979).

More recently, using an approach that they term Chemical Exchange Saturation Transfer (CEST), Balaban and coworkers (Ward et al. 2000) and the group of van Zijl (Zhou and van Zijl 2006) have shown that by saturation of a small metabolite resonance that exchanges with water it is possible to achieve a very large signal enhancement that can be 'read out' from the abundant water signal, thereby identifying the position of the resonance. A similar approach has been used to map the chemical shifts of aromatic protons of a His residue in the catalytic triad of chymotrypsinogen-A (Lauzon et al. 2011) and to image the position of an over-expressed lysine rich protein in a mouse brain (Gilad et al. 2007). The saturation transfer methodology has been extended by Clore, Torchia and coworkers who have developed an elegant ^{15}N-based 2D CEST NMR experiment, termed DEST, and used it to quantify exchange rates between amyloid β monomers and protofibrils and to obtain ^{15}N linewidths in the invisible ('dark') protofibril state (Fawzi et al. 2011). Building on this work our laboratory has recently shown that the CEST method can be used to obtain both exchange parameters and ^{15}N chemical shifts of a low populated, 'invisible state' (referred to as the excited state here) in cases where it exchanges with a visible ground conformer with rates that are often too slow to analyze quantitatively via CPMG relaxation dispersion (Vallurupalli et al. 2012). Here we extend the methodology to include slowly exchanging protein systems that are probed via $^{13}CH_3$ methyl groups. A simple 2D ^{13}C-CEST based pulse scheme is described and an application to the folding reaction of a G48M Fyn SH3 domain that has been studied extensively by CPMG relaxation dispersion NMR (Korzhnev et al. 2005; Korzhnev et al. 2004b; Mittermaier et al. 2005) is presented.

Results and discussion

Figure 1 illustrates the pulse scheme that has been developed for studies of chemical exchange in protein systems with selective ^{13}C labeling at the methyl positions. The sequence is similar to the ^{15}N DEST experiment of Clore, Torchia et al. (Fawzi et al. 2011) and the ^{15}N CEST sequence we have recently published for quantifying exchange in ^{15}N-labeled proteins (Vallurupalli et al. 2012), with a number of important differences reflecting the fact that the probe of interest here is an AX_3 and not an AX spin system. Analogous to the ^{15}N CEST scheme the magnetization transfer pathway can be described succinctly as,

$$H_Z \rightarrow 2C_{TR}H_Z \rightarrow C_Z(T_{relax}) \rightarrow 2C_{TR}H_Z(t_1) \rightarrow H_{TR}(t_2) \quad (1)$$

where t_1,t_2 are acquisition times in the indirect and direct dimensions, respectively, A_J is the $j \in \{X, Y, Z\}$ component of A magnetization, 'TR' denotes transverse magnetization and T_{relax} is a period during which a weak ^{13}C radio frequency field is applied at a specific offset from the ground state correlation. Typically a series of 2D data sets are recorded with the position of the weak ^{13}C field varied. The resulting intensities, I, of the major state correlations are plotted as a function of the offset of the weak field, generating dips in I that correspond to the positions of the ground and excited state resonances. In the case of an AX spin system it is straightforward to prepare longitudinal A magnetization immediately prior to the application of the CEST B_1 field, $H_Z \rightarrow 2C_{TR}H_Z \rightarrow C_Z$, with no loss in sensitivity outside of the normal decay due to relaxation. By contrast, for a $^{13}CH_3$ group transfer from transverse ^{1}H to in-phase ^{13}C magnetization does not go to completion because during the delay between points a and b in the scheme of Fig. 1 evolution proceeds according to

$$\begin{aligned} 2C_YH_Z \rightarrow & -3\sin\theta_b\cos^2\theta_b C_X \\ & + (\cos^3\theta_b - 2\sin^2\theta_b\cos\theta_b)2C_YH_Z \\ & + (\sin^3\theta_b - 2\sin\theta_b\cos^2\theta_b)\sum_{i,j;i\neq j} 4C_XH_Z^iH_Z^j \\ & - (3\sin^2\theta_b\cos\theta_b)8C_YH_Z^1H_Z^2H_Z^3 \end{aligned} \quad (2)$$

with anti-phase ^{13}C magnetization transferred only partially into the desired C_X coherence (Sorensen et al. 1983). In Eq. [2] H_Z is the total ^{1}H Z-magnetization and $\theta_b = 2\pi J_{HC}\tau_b$ where J_{HC} is the one-bond ^{1}H–^{13}C coupling constant. ^{13}C singly and triply anti-phase magnetization are eliminated by the subsequent action of gradient g4 and magnetization denoted by $4C_XH_Z^iH_Z^j$ is suppressed by choosing θ_b such that $1–3\cos^2\theta_b = 0$. Residual doubly anti-phase magnetization is partially eliminated by the application of a ^{1}H 90° pulse and gradient g4. Optimal spectral sensitivity is achieved by setting $\tau_c = \frac{\arccos(\sqrt{2/3})}{2\pi J_{HC}}$ that maximizes the transfer function from C_Y to $2C_XH_Z$ for an AX_3 group during the final reverse INEPT element. It can be shown that, neglecting relaxation effects, the sensitivity of the experiment is reduced by a factor of approximately 3 relative to a standard HSQC sequence. A similar scheme has recently been described for off-resonance ^{13}C $R_{1\rho}$ measurements and the interested reader is referred there for further details (Baldwin and Kay 2012).

In order to first test the methodology we have made use of a highly deuterated Ileδ1-[$^{13}CH_3$], Leu, Val-[$^{13}CH_3$,$^{12}CD_3$] sample of protein L, a 63 residue protein that does not show evidence of conformational exchange

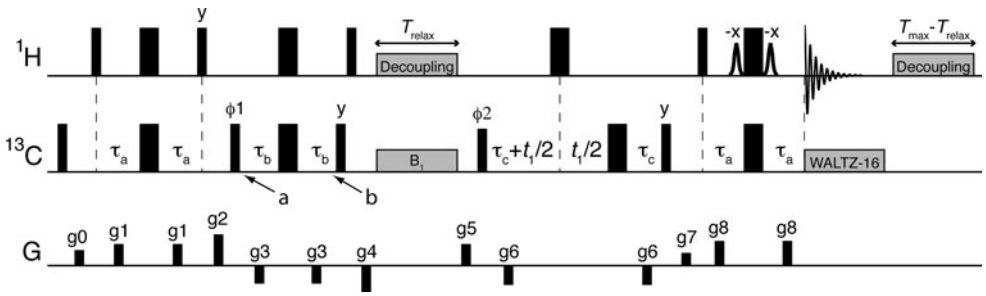

Fig. 1 Pulse scheme of the ^{13}C-methyl CEST experiment for studying slowly exchanging protein systems. ^{1}H and ^{13}C 90° (180°) pulses are shown as narrow (wide) *black bars* and are applied at the highest possible power levels. The shaped 90° ^{1}H pulses are water-selective (~1.5 ms). All pulse phases are assumed to be x, unless indicated otherwise. The ^{13}C transmitter is positioned in the center of the methyl region except for the duration of the weak B_1 field (~10–30 Hz), where it is placed at the desired offset. ^{1}H decoupling during the T_{relax} element is achieved using a (~5 kHz) $90_x240_y90_x$ composite pulse train (Levitt 1982). The phase cycling used is as follows: $\phi1 = x, -x$; $\phi2 = 2\{x\}, 2\{-x\}$; receiver = x, 2 {−x}, x. Quadrature detection in the indirect dimension is obtained via States-TPPI of $\phi2$ (Marion et al. 1989). The delays used are: $\tau_a = 1.8$ ms; $\tau_b = 1.217$ ms; $\tau_c = 784$ µs. Gradient strengths, G/cm (length in ms) are: g0 = 7.5 (1.0); g1 = 10.0 (0.5); g2 = 15.0 (0.8); g3 = −4.0 (0.6); g4 = −16.0 (1.0); g5 = 10.0 (0.7); g6 = −12.0 (0.3); g7 = 5.0 (0.5); g8 = 15.0 (0.3). ^{13}C decoupling during acquisition is achieved via WALTZ-16 (Shaka et al. 1983). A ^{1}H decoupling block of length $T_{max} - T_{relax}$ (where T_{max} is the maximum T_{relax} delay used) is applied at the end of acquisition so that the extent of heating is constant over all measurements, including for the data set recorded with $T_{relax} = 0$. A recycle delay of 2.0 s was used between scans

on a millisecond time-scale (Korzhnev et al. 2004a). It is noteworthy that deuteration is not a requirement of the method, nor are samples where one of the two isopropyl methyl groups is $^{12}CD_3$, however it is important that ^{13}C methyl spins of interest are not attached to ^{13}C carbons. A series of ^{13}C–^{1}H 2D HSQC data sets were recorded as a function of the position of the ^{13}C B_1 field, ranging from 8.7 to 28.6 ppm, applied during the delay T_{relax}. Only a single "peak" is expected in each profile corresponding to the resonance position of a specific methyl group. The methyl ^{13}C–^{1}H correlation map of protein L is shown in Fig. 2a, with CEST profiles for the 3 peaks highlighted (red) indicated in Fig. 2b–d, recorded at 11.7 T with a ^{13}C B_1 field of 30 Hz and $T_{relax} = 400$ ms. Very 'clean' CEST profiles are obtained, as expected. It is worth noting that ^{1}H decoupling during the T_{relax} element is achieved using a $90_x240_y90_x$ composite pulse train (Levitt 1982) that generates decoupling sidebands at a distance of $\pm 1/(2pw_{INV})$ from the major peak, where pw_{INV} is the length of the composite inversion pulse (1.17/^{1}H field). We have shown previously that such sidebands are very small and only (barely) observed on very concentrated samples (tested on a 4 mM sample) (Vallurupalli et al. 2012). Using a typical ^{1}H decoupling field of 5 kHz places the sidebands ±2,140 Hz from the central peak, well outside of the range where the excited state resonance positions would lie (<~ ± 2 ppm from the ground state correlation).

Having established the utility of the method we next turned to studies of the G48M Fyn SH3 domain, previously shown by our laboratory to fold on the millisecond time-scale (Korzhnev et al. 2004b; Mittermaier et al. 2005). A highly deuterated Ileδ1-[$^{13}CH_3$], Leu, Val-[$^{13}CH_3$,$^{13}CH_3$] sample was used in the analysis, that had been previously employed in CPMG relaxation dispersion studies on this system (Mittermaier et al. 2005) and a temperature of 1 °C was chosen so as to place the kinetics into a regime which is particularly well suited for the CEST methodology (typically < 200–300 s^{-1}). Figure 3a shows an aliased ^{13}C,^{1}H HSQC spectrum (peaks in green aliased once, * denotes double aliasing), 14.0 T, 1 °C, with CEST profiles for correlations highlighted in red indicated in Fig. 3b–d, $T_{relax} = 300$ ms. A pair of experiments, corresponding to B_1 field strengths of 15 and 30 Hz, was recorded and profiles from both are illustrated in the Figures. It is clear that in addition to the major peak that is always observed in CEST spectra a second 'correlation', corresponding to an exchanging minor state is also noted. As discussed previously (Vallurupalli et al. 2012) and evident in the present set of data, peak linewidths increase with applied B_1 field since a larger field perturbs longitudinal magnetization further off-resonance than a correspondingly weaker field. This is a potential drawback in cases where $\Delta\varpi$ is small (for example, Fig. 3b). By contrast, the size of the dips corresponding to the resonance positions of the nuclei in the excited state, increase with B_1 field, a distinct advantage. We therefore prefer to record data sets with several B_1 fields, typically between 10 and 30 Hz, that also greatly facilitates extraction of 'natural' line-widths of the excited state peaks.

Only 1 set of additional peaks was observed in CEST profiles of the G48M Fyn SH3 domain. Therefore, all of the data (2 B_1 fields and 18 residues) have been simultaneously fitted (solid lines) to a two-site exchange model, $E \underset{k_{GE}}{\overset{k_{EG}}{\leftrightarrow}} G$, to obtain the population of the excited state $p_E = 4.4$ % and $k_{ex} = k_{EG} + k_{GE} = 48 \pm 1$ s^{-1}. The fitting details are given in Materials and Methods. In addition

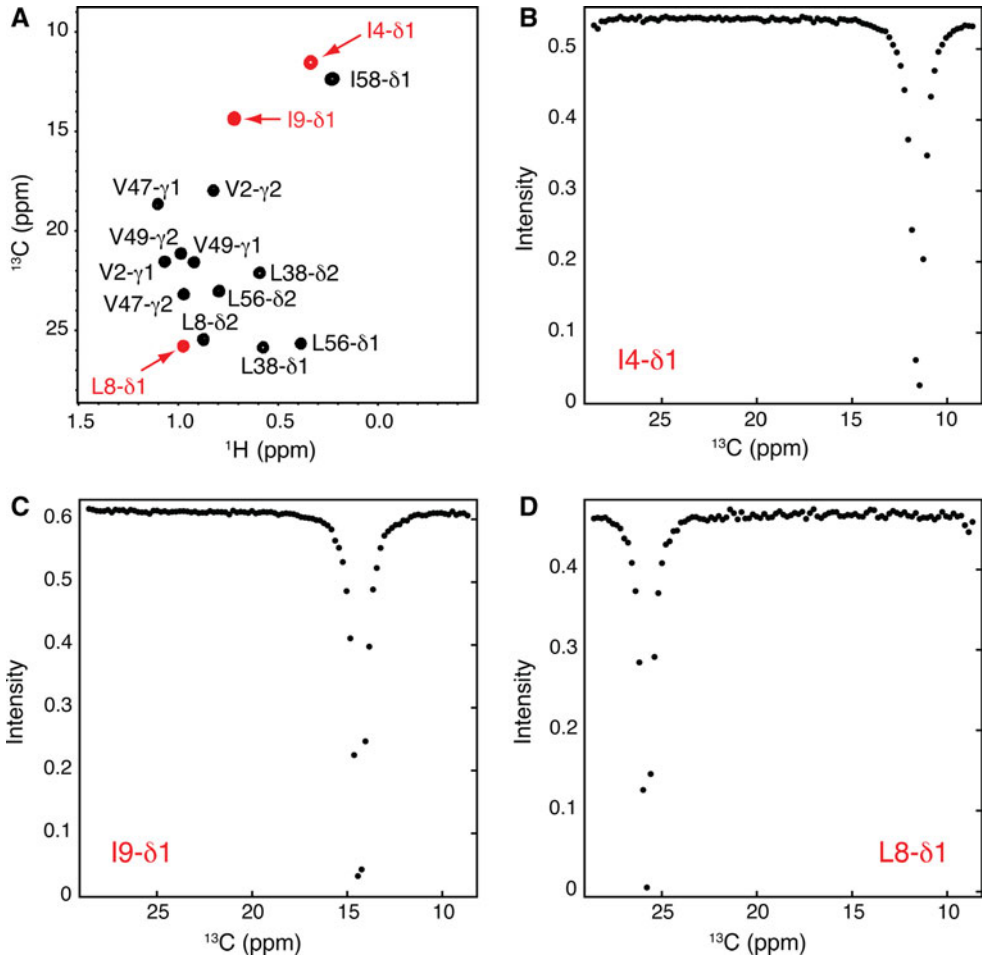

Fig. 2 **a** Methyl ^{13}C–^{1}H spectrum of protein L, 25 °C, 11.7T. Residues highlighted in *red* are those for which dispersion profiles are illustrated in (**b**–**d**). **b**–**d** ^{13}C-methyl CEST intensity profiles of methyl groups I4-δ1 (**b**), I9-δ1 (**c**), L8-δ1 (**d**) obtained using the scheme of Fig. 1 with $T_{relax} = 400$ ms and $\gamma B_1/2\pi = 30$ Hz

to the exchange parameters values for signed chemical shift differences between states E and G, $\Delta\varpi^{C13}_{CEST} = \varpi^{C13}_{E} - \varpi^{C13}_{G}$, are also generated. These are plotted versus predicted $\Delta\varpi^{C13}$values in Fig. 4a, assuming that the excited state shifts correspond to random coil values and an excellent correlation is obtained. The inset to the figure shows the correlation between (k_{ex}, p_E) values generated on the basis of per-residue fits of those residues for which very well resolved dips for the minor state were observed in CEST profiles. With the exception of 1 residue there is a very close clustering of values, consistent with the CEST data reporting on a single exchange process.

While the nature of the excited state cannot be confirmed from this limited data it is consistent with a conformation where the methyl containing side-chains are highly dynamic, likely forming only limited contacts with other residues. In order to further probe the nature of the excited state we have recorded ^{15}N CEST experiments, following the approach described in detail previously (Vallurupalli et al. 2012). The data were very well fit to a two-site exchange model and exchange parameters (k_{ex}, p_E) from global fits of the ^{13}C and ^{15}N data are in excellent agreement (compare the blue, ^{15}N, and red ^{13}C circles in the Fig. 4a inset, centered at (k_{ex}, p_E) = (4.1 %, 54 s^{-1}) and (4.4 %, 48 s^{-1}), respectively). The extracted $\Delta\varpi^{N15}_{CEST}$values (1 °C) are highly correlated with $\Delta\varpi^{N15}_{U-N} = \varpi^{N15}_{U} - \varpi^{N15}_{N}$, the difference in chemical shifts between unfolded and native states of the Fyn SH3 domain, determined from fits of a set of 6 CPMG relaxation dispersion data sets (25 °C), Fig. 4b, that have been published previously (Korzhnev et al. 2005). This strong correlation establishes that the excited state probed by the CEST data is, indeed, unfolded. It is noteworthy that the backbone amide ^{1}H and ^{15}N CPMG data that have been recorded for the Fyn SH3 domain are much better fit to a model of 3-site exchange (twofold reduction in χ^2), providing strong evidence for the presence of a folding intermediate that we were able to establish as being on-pathway (Korzhnev et al. 2004b; Korzhnev et al. 2005). In addition to $\Delta\varpi^{N15}_{U-N}$ values extracted from the CPMG fits so too were the differences between chemical shifts of ^{15}N spins in the native and intermediate states, $\Delta\varpi^{N15}_{I-N} = \varpi^{N15}_{I} - \varpi^{N15}_{N}$ (Korzhnev et al. 2005). These however, do not agree with the $\Delta\varpi^{N15}$ values from CEST, Fig. 4b inset.

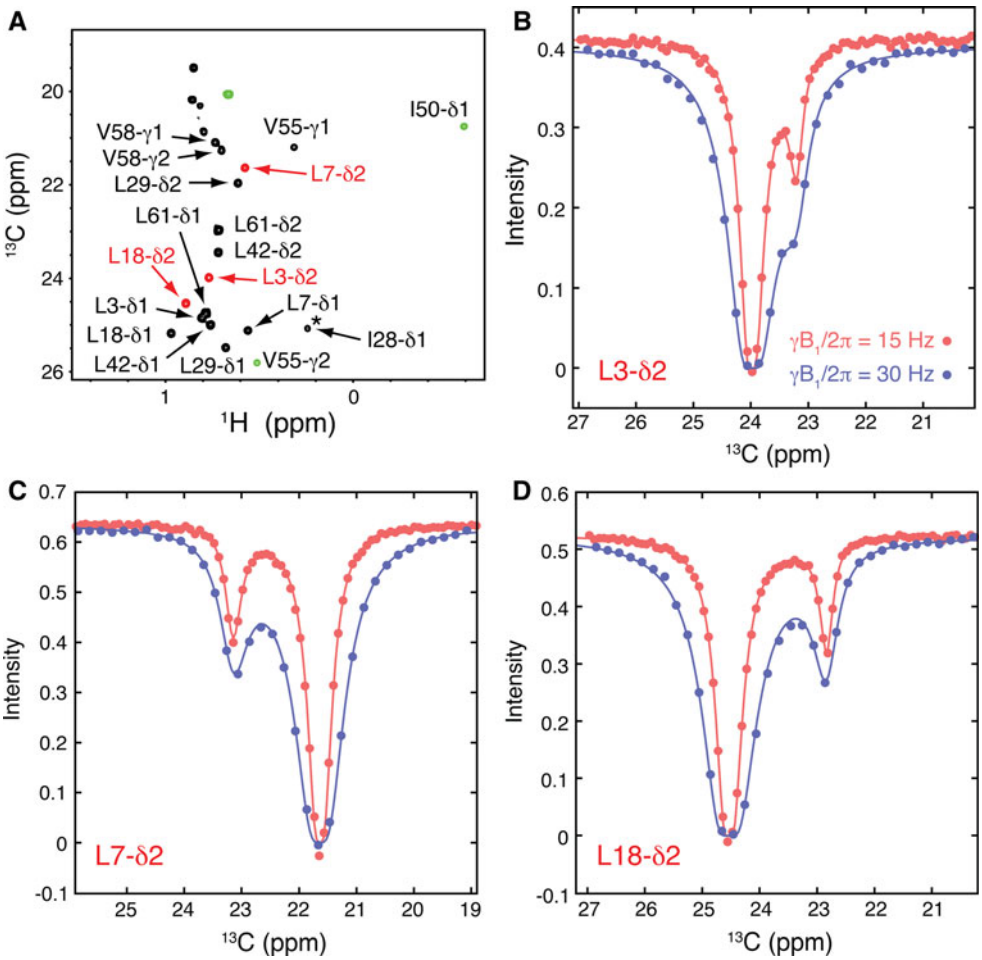

Fig. 3 **a** Methyl ^{13}C–^{1}H spectrum of G48M FynSH3, recorded at 1 °C, 14.0 T. *Peaks* aliased a single time (twice) are in *green* (*star*). Profiles in (**b**, **c**, **d**) derive from residues whose *cross-peaks* are highlighted in *red*. **b–d** ^{13}C-methyl CEST intensity profiles of methyl groups L3-δ2 (**b**), L7-δ2 (**c**), L18-δ2 (**d**) recorded using the sequence of Fig. 1 with T_{relax} = 300 ms and a B_1 field strength = 15 (*red*) and 30 (*blue*) Hz. Experimental data points are indicated with *circles* along with best fits of the data (*solid lines*) obtained from simultaneous analysis of all profiles recorded for the pair of B_1 values. The main dip derives from the major state while the secondary, smaller dip comes from the "invisible" minor state

In contrast to the ^{15}N CPMG data, side-chain methyl ^{13}C CPMG data were equally well fit by a 2-site model, reflecting the fact that methyl ^{13}C chemical shifts of the intermediate are uniformly close to those of the unfolded state (Mittermaier et al. 2005). The ^{13}C methyl CEST data could also be well fit to a 2-site exchange scheme as described above. Our CEST data do, however, provide evidence for an additional state likely in moderately fast exchange with the excited state. Figure 5 plots the fitted ^{13}C R_2 values for the excited (red) and ground (blue) states. Notably, for many residues very similar transverse relaxation rates are obtained, but for others there are sizable differences. The increased rates for the excited state can be explained by additional exchange processes, beyond the primary two-site interchange that is fitted explicitly. It is not possible to say what this extra state might be based on the limited data obtained here.

In summary, we have presented a simple ^{13}C CEST pulse scheme for studies of protein exchanging systems using methyl groups as probes. The experiment, focusing on hydrophobic side-chains localized to the interior of proteins, is complementary to ^{15}N CEST methodology that has been developed for investigating backbone positions in proteins. We have shown that high quality methyl CEST spectra can be obtained and that the extracted exchange parameters from them are in excellent agreement with those generated via ^{15}N-based approaches. The methodology further extends the assortment of NMR experiments that are available for studies of exchanging protein systems.

Materials and methods

Protein Production: A highly deuterated Ileδ1-[^{13}CH$_3$], Leu, Val-[^{13}CH$_3$,^{12}CD$_3$] sample of protein L was prepared as described previously (Mittermaier and Kay 2001). The concentration of the protein was 1.2 mM dissolved in 50 mM sodium phosphate, 0.05 % NaN_3, pH 6.0 10 % D_2O buffer. A Fyn tyrosine kinase SH3 domain (chicken isoform) sample was generated as described by Mettermaier et al. (2005), with a Gly to Met mutation at position 48. The sample was prepared with ^{13}C and ^{1}H incorporated into the C$^{\delta}$ methyl groups of Leu and Ile, and the C$^{\gamma}$ methyls of Val residues (Goto et al. 1999); the side-chains of Phe and Trp were fully protonated, for reasons that are not germane to the present set of experiments, with all other positions

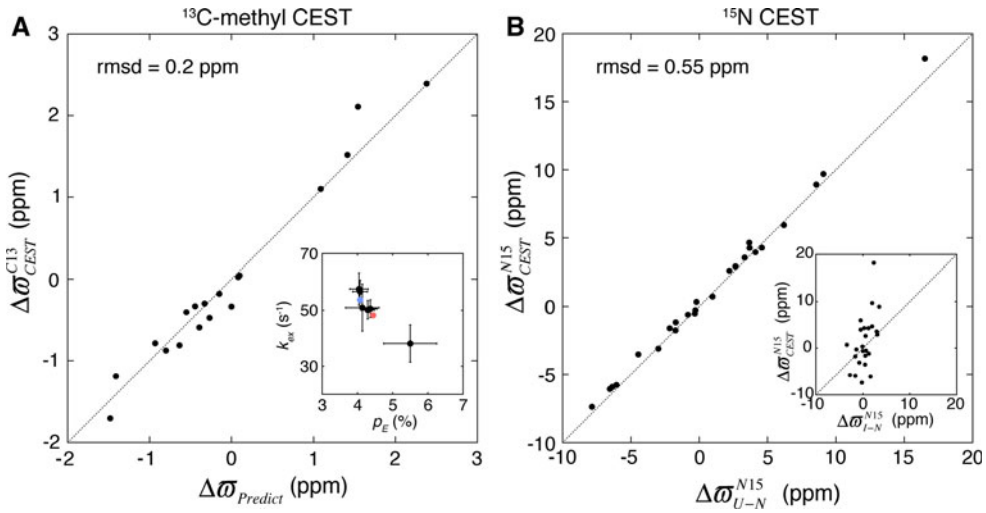

Fig. 4 The minor state is random-coil like. **a** Correlation plot of ^{13}C-methyl chemical shift differences, $\Delta\varpi^{C13}_{CEST} = \varpi^{C13}_{E} - \varpi^{C13}_{G}$, of the G48M FynSH3 domain obtained from analysis of CEST derived data (Y axis) versus predicted shift differences, $\Delta\varpi_{\text{Predict}}$, assuming that the excited state is unfolded (X axis). Random coil chemical shifts values used in the calculation of $\Delta\varpi_{\text{Predict}}$ were obtained from Wishart and coworkers (Wishart et al. 1995). Values of $\Delta\varpi^{C13}_{CEST}$ were extracted from the global fit of CEST intensity profiles recorded at 1 °C, 14.0 T with 15 Hz and 30 Hz radio frequency fields. An offset of 0.2 ppm was applied to $\Delta\varpi_{\text{Predict}}$values to produce the fit shown. Values of (k_{ex}, p_E) obtained on a per-residue basis for those residues with $|\Delta\varpi^{C13}_{CEST}| > 0.35$ ppm are shown in the inset (*black*) along with exchange parameters from global fits of ^{13}C (*red*) or ^{15}N (blue) CEST data. **b** ^{15}N chemical shift differences, $\Delta\varpi^{N15}_{CEST}$, extracted from fits of ^{15}N CEST data (Y axis) are highly correlated with $\Delta\varpi^{N15}_{U-N} = \varpi^{N15}_{U} - \varpi^{N15}_{N}$(X axis), but not with $\Delta\varpi^{N15}_{I-N} = \varpi^{N15}_{I} - \varpi^{N15}_{N}$, inset, establishing that the excited state probed by CEST is unfolded. Values of $\Delta\varpi^{N15}_{U-N}$ and $\Delta\varpi^{N15}_{I-N}$ were obtained from analyses of CPMG data recorded previously (Korzhnev et al. 2005), while $\Delta\varpi^{N15}_{CEST}$were extracted from the global fit of ^{15}N CEST intensity profiles recorded at 1 °C, 11.7T, B_1 field = 15 Hz

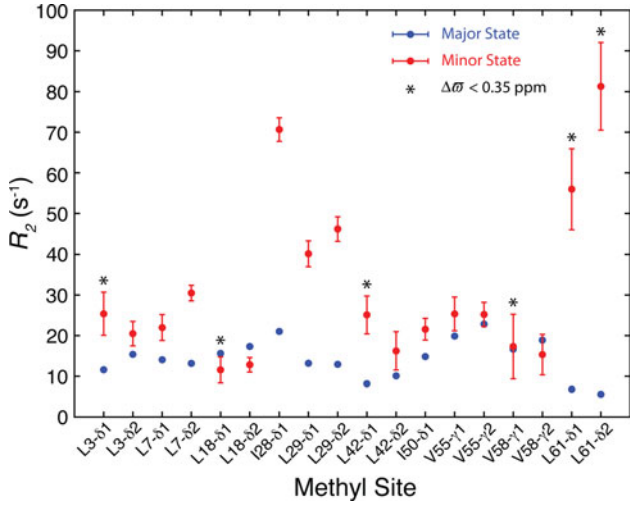

Fig. 5 ^{13}C-methyl transverse relaxation rates, R_2, of the major (*blue*) and minor (*red*) states for the G48M Fyn SH3 domain extracted from fits of CEST profiles recorded at 1 °C, 14.0 T, B_1 field strengths of 15 and 30 Hz as a function of methyl group. Residues for which the minor state *peak* is poorly resolved from the major correlation in CEST profiles, and hence R_2 values for the excited state are error prone, ($\Delta\varpi^{C13}_{CEST}$<0.35 ppm) are indicated by an *asterisk*

^{2}H and ^{12}C. The protein concentration was ≈1 mM and the sample contained 50 mM sodium phosphate, 1 mM EDTA, 1 mM NaN_3, 90 %/10 % H_2O/D_2O, pH 7.0.

NMR Spectroscopy and Data Analysis: ^{13}C CEST data on protein L were obtained at 25 °C, 11.7T, using a single ^{13}C B_1 field strength of 28 Hz applied during an interval T_{relax} = 0.4 s. A 4.9 kHz ^{1}H decoupling field was employed during this time. A set of 101 2D spectra were recorded in steps of 25 Hz with the position of the weak B_1 field ranging from 8.7-28.6 ppm. Each data set was recorded with (t_{1max}, t_{2max}) = (11.7 ms, 64 ms), 8 scans/FID and a repetition delay of 2.0 s for a net acquisition time of 0.33 h and a total time of 34 h for the complete 2D series. Fyn SH3 ^{13}C data were recorded at 1 °C, 14.0 T, using a pair of B_1 fields, 15 and 30.5 Hz. 191 data sets were obtained for B_1 = 15 Hz, with offsets ranging from 7.1 to 15.5 ppm (50 spectra, 25 Hz steps) and from 15.5 to 27 ppm (141 spectra, 12.5 Hz steps); 100 spectra were recorded from 7.1 to 27 ppm in 30 Hz increments for B_1 = 30.5 Hz. Each 2D data set was obtained with (t_{1max}, t_{2max}) = (30.5 ms, 64 ms), 4 scans/FID and a repetition delay of 2.0 s corresponding to a total measuring time of 36.5 (B_1 = 15 Hz) and 19 (B_1 = 30.5 Hz) h for each 2D series. In order to validate the exchange parameters obtained from the ^{13}C CEST experiment and to establish that the Fyn SH3 domain excited state probed by the CEST experiment is the unfolded conformation, an ^{15}N CEST data set was acquired at 11.7 T. It was comprised of 61 2D spectra (from 104.2 to 133.8 ppm in 25 Hz steps), B_1 = 16 Hz, T_{relax} = 0.5 s. Each spectrum was recorded with 8 scans/FID, (t_{1max}, t_{2max}) = (35 ms, 64 ms), and a repetition delay of 2.0 s corresponding to a total time of

20 h for the full 2D series. Each CEST data set included a plane recorded with $T_{relax} = 0$ that allows a robust estimate of the longitudinal relaxation rate of the ground state. Weak B_1 fields applied during T_{relax} were calibrated according to the procedure of Guenneugues et al. (1999).

It is worth noting that although highly deuterated samples were used in the present study (see above), the level of deuteration has little impact on the ^{13}C B_1 fields chosen to observe the CEST effect. Moreover, although the 'sharpness' of the dips in the CEST profile is affected significantly by the size of the ^{13}C B_1 field (see text) and by the 'natural' ^{13}C linewidths of the peaks in question, there is little influence from the level of deuteration. Deuteration is thus not expected to affect the CEST profiles in any meaningful way.

All data were fit to the Bloch-McConnell equations describing the evolution of magnetization (McConnell 1958) as discussed in detail previously (Vallurupalli et al. 2012), with fitting parameters $\{k_{\rm ex}, p_E, \varpi_E, R_1^G, R_2^G, R_2^E, I_o\}$, where I_o is an initial intensity that is residue specific. Data sets obtained with multiple B_1 fields were analyzed simultaneously and all residues were included in the analysis, including those for which well-resolved excited state dips were not obtained. In the analysis of the CEST data we did not explicitly modify the Bloch-McConnell equations to take into account ^{1}H-^{13}C cross-correlated spin relaxation. That is, the description of the time-evolution of magnetization includes only the X, Y, Z components of each of the exchanging states and does not include the exchange of (C_X, C_Z) to doubly anti-phase $(4C_XH_Z^iH_Z^j, 4C_ZH_Z^iH_Z^j)$ components (Vold and Vold 1976; Werbelow and Grant 1977). Cross-correlation effects can be minimized, but not eliminated, by ensuring that at the start of the CEST relaxation period only in-phase ^{13}C magnetization is present, as is done in the present experiment. The relaxation rates extracted do depend on T_{relax} (non-exponential decay), and are slightly elevated from what they would be if cross-correlated relaxation were included. To establish that accurate exchange parameters and chemical shift differences can be extracted from the experimental data we have computed sets of simulated CEST profiles for $p_E \in \{1, 2, 3, 4, 5\}$% and $k_{ex} \in \{20, 50, 100, 200\}$s^{-1}, with each data set comprised of 12 profiles generated using experimental $\Delta\varpi_{CEST}^{C13}$ values extracted from the analysis of the Fyn SH3 data ($\Delta\varpi_{CEST}^{C13} \geq 0.35$ ppm). CEST curves were calculated using modified Bloch-McConnell equations that explicitly include $4C_XH_Z^iH_Z^j, 4C_ZH_Z^iH_Z^j$ for the ground and excited states and then fit to equations that neglect cross-correlation. A very high correspondence between input and fitted values of (p_E, k_{ex}) was obtained, with average discrepancies of 2.7 and 3.7 %, respectively, with the largest discrepancies obtained for $(p_E, k_{ex}) = (2\ \%, 20\ \text{s}^{-1})$ where values of 10.7 and 16.1 % were calculated. Of note, the errors are largest for the smallest k_{ex} values. It is important to emphasize the excellent agreement between (p_E, k_{ex}) values from fits of ^{15}N $(4.1 \pm 0.1\ \%, 53.7 \pm 3.4\ \text{s}^{-1})$ and ^{13}C $(4.4 \pm 0.1\ \%, 48.1 \pm 1.3\ \text{s}^{-1})$ CEST experimental data recorded on the Fyn SH3 domain that further establishes that cross-correlated spin relaxation can be neglected in fits of the methyl ^{13}C CEST data.

Acknowledgments G.B. acknowledges the Canadian Institutes of Health Research (CHIR) for a post-doctoral fellowship. This work was supported by grants from the CIHR and the Natural Sciences and Engineering Research Council of Canada. L. E. K. holds a Canada Research Chair in Biochemistry.

References

Alger JR, Shulman RG (1984) NMR studies of enzymatic rates in vitro and in vivo by magnetization transfer. Q Rev Biophys 17:83–124

Baldwin AJ, Kay LE (2012) Measurement of the signs of methyl 13C chemical shift differences between interconverting ground and excited protein states by R1rho: an application to αB crystallin. J Biomol NMR 53:1–12

Cayley PJ, Albrand JP, Feeney J, Roberts GC, Piper EA, Burgen AS (1979) Nuclear magnetic resonance studies of the binding of trimethoprim to dihydrofolate reductase. Biochemistry 18:3886–3895

Fawzi NL, Ying J, Ghirlando R, Torchia DA, Clore GM (2011) Atomic-resolution dynamics on the surface of amyloid-beta protofibrils probed by solution NMR. Nature 480:268–272

Forsen S, Hoffman RA (1963) Study of moderately rapid chemical exchange reactions by means of nuclear magnetic double resonance. J Chem Phys 39:2892–2901

Gilad AA, McMahon MT, Walczak P, Winnard PT Jr, Raman V, van Laarhoven HW, Skoglund CM, Bulte JW, van Zijl PC (2007) Artificial reporter gene providing MRI contrast based on proton exchange. Nat Biotechnol 25:217–219

Goto NK, Gardner KH, Mueller GA, Willis RC, Kay LE (1999) A robust and cost-effective method for the production of Val, Leu, Ile (δ1) methyl-protonated ^{15}N-,^{13}C-,^{2}H-labeled proteins. J Biomol NMR 13:369–374

Guenneugues M, Berthault P, Desvaux H (1999) A method for determining B1 field inhomogeneity. Are the biases assumed in heteronuclear relaxation experiments usually underestimated? J Magn Reson 136:118–126

Gupta RK, Redfield AG (1970) Double nuclear magnetic resonance observation of electron exchange between ferri- and ferrocytochrome c. Science 169:1204–1206

Korzhnev DM, Kloiber K, Kanelis V, Tugarinov V, Kay LE (2004a) Probing slow dynamics in high molecular weight proteins by methyl-TROSY NMR spectroscopy: application to a 723-residue enzyme. J Am Chem Soc 126:3964–3973

Korzhnev DM, Salvatella X, Vendruscolo M, Di Nardo AA, Davidson AR, Dobson CM, Kay LE (2004b) Low-populated folding intermediates of Fyn SH3 characterized by relaxation dispersion NMR. Nature 430:586–590

Korzhnev DM, Neudecker P, Mittermaier A, Orekhov VY, Kay LE (2005) Multiple-site exchange in proteins studied with a suite of six NMR relaxation dispersion experiments: an application to the folding of a Fyn SH3 domain mutant. J Am Chem Soc 127:15602–15611

Lauzon CB, van Zijl P, Stivers JT (2011) Using the water signal to detect invisible exchanging protons in the catalytic triad of a serine protease. J Biomol NMR 50:299–314

Levitt MH (1982) Symmetrical composite pulse sequences for NMR population-inversion. 2. Compensation of resonance offset. J Magn Reson 50:95–110

Marion D, Ikura M, Tschudin R, Bax A (1989) Rapid recording of 2D NMR spectra without phase cycling. Application to the study of hydrogen exchange in proteins. J Magn Reson 85:393–399

McConnell HM (1958) Reaction rates by nuclear magnetic resonance. J Chem Phys 28:430–431

Mittermaier A, Kay LE (2001) Chi1 torsion angle dynamics in proteins from dipolar couplings. J Am Chem Soc 123:6892–6903

Mittermaier A, Korzhnev DM, Kay LE (2005) Side-chain interactions in the folding pathway of a Fyn SH3 domain mutant studied by relaxation dispersion NMR spectroscopy. Biochemistry 44:15430–15436

Shaka AJ, Keeler J, Frenkiel T, Freeman R (1983) An improved sequence for broadband decoupling: WALTZ-16. J Magn Reson 52:335–338

Sorensen OW, Eich GW, Levitt MH, Bodenhausen G, Ernst RR (1983) Product operator formalism for the description of NMR pulse experiments. Prog NMR Spectrosc 16:163–192

Vallurupalli P, Bouvignies G, Kay LE (2012) Studying 'invisible' excited protein states in slow exchange with a major conformation. J Am Chem Soc 134:8148–8161

Vold RR, Vold RL (1976) Transverse relaxation in heteronuclear coupled spin systems: AX, AX2, AX3. AXY J Chem Phys 64:320–332

Ward KM, Aletras AH, Balaban RS (2000) A new class of contrast agents for MRI based on proton chemical exchange dependent saturation transfer (CEST). J Magn Reson 143:79–87

Werbelow LG, Grant DM (1977) Intramolecular dipolar relaxation in multispin systems. Adv Magn Reson 9:189–299

Wishart DS, Bigam CG, Holm A, Hodges RS, Sykes BD (1995) 1H, 13C and 15N random coil NMR chemical shifts of the common amino acids. I. Investigations of nearest-neighbor effects. J Biomol NMR 5:67–81

Zhou JY, van Zijl PCM (2006) Chemical exchange saturation transfer imaging and spectroscopy. Prog Nucl Magn Reson Spectrosc 48:109–136